



Study on Gas Induction and Comparison of Power Consumption of Gas Inducing Mechanically Agitated Contactors with the Gas Sparging Mechanically Agitated contactors

Eldho Abraham

Department of Chemical Engineering, St. Joseph's College of Engineering, Chennai, Tamil Nadu, India

Abstract : Gas Inducing Mechanically Agitated Contactors (GIMAC) are now gaining importance as its economical, environmental and process benefits as concern. This paper, the air induction mechanism in GIMACs has been elaborated. The main endeavour here is to make a comparison of the energy consumption of the GIMAC with the conventional mechanically agitated sparged gas contactors. In the experimentation water has been used as the medium and the induced air flow rates at various impeller submersion depths and different rotational speed have been measured along with the resulting gas holdup and respective energy consumption. The relation between the rotational speed and the induced gas flow rate has been investigated. In addition to this the effect of the impeller submersion depth on the gas induction rate and the gas holdup of the GIMAC has been analyzed. The effect of the induced gas flow rate on the gas holdup has also been studied. The performance of the conventional sparging system is also measured with respect to the same above parameters. The both performance have been compared in terms of power consumption and gas holdup.

Key words: Gas inducing mechanically agitated contactor, Mechanically agitated sparged gas contactors, Gas holdup, Rate of gas induction, Dispersed gas phase.

1. Introduction

A gas inducing mechanically agitated contactor or reactor is basically a gas-liquid contacting equipment with or without the presence of solids which lacks the bottom sparger for air admission and instead it sucks the gas through the hollow rotor - impeller when it rotates due to the reduction of pressure inside the liquid. The simple classification given to the air inducing reactors is dead end systems and open end systems. A typical dead end system recycles the unreacted gas internally through the reactor and ensures effective solute gas utilization. In contrast the open end systems are in contact with the atmosphere and the solute gas will not be readily available for the recycle or virtually there will be no recycle of the solute gas. The open end systems are extensively used when air is being used as the gaseous reactant where a recycle operation is not necessary. In chemical process industries, gas-liquid contacting with or without solids is one of the most important operations. In many of the cases, the per pass conversion of gas is fairly low and is also desirable to recycle the unreacted gas back to the reactor because the gas may be highly toxic, may pose safety problems or of economical considerations. Typical examples include alkylation, ethoxylation, hydrogenation, chlorination, ammonolysis, oxidation, and so forth. In such a situation the importance of a reactor system which recycles the excess unreacted gas without an external compressor loop is more significant and a kind of that system can ensure plant and environmental safety into a larger extend in an economical way. The use of gas inducing reactors gaining industrial importance nowadays as it is eliminating the wear and tear problems with the sparger holes and the blockage apart from other economical and environmental benefits. The absence of the expensive

compressor in the external loop make a gas inducing mechanically agitated contactor (GIMAC) less capital and less power consuming and an effective reactor system for gas liquid solid contacting. These kinds of contactors can also produce higher mass and heat transfer rates when comparing with its counterparts.

The gas induction rate is closely related to the rotational speed of the impeller. The impeller speed increases, the gas induction rate increases. The relation between the rotational speed and the gas induction rate has been studied in this work. The submersion depth is having a highly influencing effect on the gas induction rate and the gas holdup. So the effect of same on gas induction rate and gas holdup has been analyzed. The role of the gas flow rate in influencing the gas holdup has been investigated. In addition to this the real effort has been put to compare the power consumption of the both types of the gas liquid contactors. The comparison is made in terms of the ability of the system to hold the solute gas in the form of holdup and the power consumption for a required performance.

1.1 Basic Constructional Features of Gas Inducing Mechanically Agitated Contactor

A hollow impeller mounted on a hollow shaft makes the gas inducing system distinct from the gas sparging systems. The hollow impeller will be provided with orifices on its blade surface and these orifices will be connected to the hollow shaft through the internal channels of the blades. There will be an opening in the upper end of the hollow shaft and this opening make the way for the admission of the gas. These constitute the gas pathway for the induced gas from the headspace into the liquid. The shaft will be connected to a motor for providing the necessary mechanical drive. The schematic representation of a typical gas inducing system is given in the figure 1.

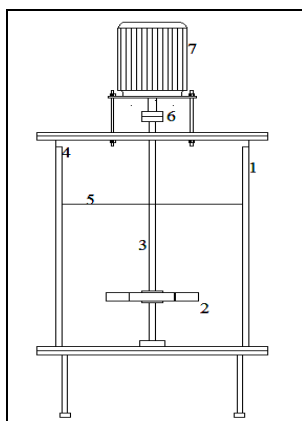


Figure:1 Gas inducing mechanically agitated contactor

1. Tank
2. Gas inducing impeller
3. Hollow shaft
4. Baffles
5. Liquid level
6. Coupling

2.Previous Work

2.1Mechanism of Gas Induction

The mechanism of the gas induction has depicted in detail in various literatures^{1,8,9}. Due to the hydrostatic equilibrium, the water level inside the hollow impeller equals with the water level in the tank when the impeller is in rest. Let $P(\theta)$ be the pressure acting over the orifice at any angular position due to the static head and P_o be the head space pressure. When the impeller starts to rotate, it imparts the necessary kinetic energy to the liquid, which creates a corresponding movement in the liquid. As a result the static pressure head offered by the liquid gradually reduces with respect to the increase in impeller speed. At a particular point of liquid velocity, the pressure acting on any angular position of the orifice is reduced to a level which is lower than the head space pressure. Due to this pressure difference, the gas at the head space flows to the liquid through the hollow channel and this caused the gas induction. The beginning of the gas induction will be at a

point when the P_o equals the $P(\theta)$. The impeller speed at this instance is referred as critical impeller speed of the gas induction process. It has been found from the various literatures that the centrifugal force acting on the gas due to the impeller rotation have negligible effect on the gas induction. There is considerable pressure loss due to the flow through the hollow shaft, channel inside the impeller blade and the orifice due to frictional and orifice loss⁵. In addition to this the exit of the gas from the orifice front to the working liquid in the form of bubbles also expends energy causing a drop in pressure^{12,13}. These pressure drops together can be accounted as total pressure drop and can be denoted as ΔP_T . The driving force for the gas induction through the orifice is the pressure difference between the head space pressure and the pressure acting on the orifice at any angular location. The gas induction occurs when the difference between the P_o and the $P(\theta)$ slightly exceeds the value of ΔP_T . As far as the gas induction in a GIMAC as concern the hydrodynamics of the systems serves an important role in and this deals with various systems behaviours like the pressure reduction in the liquid, critical gas induction speed, power consumption, gas hold up, mechanism of gas bubble formation, ejection of the bubbles from the orifice, bubble size, residence time and distribution of the bubbles in the liquid etc. In addition to this, the various geometrical and non geometrical parameters of the system have a strong influence on these behaviours¹⁰.

2.2 Gas induction rate

Gas induction rate increases as the rpm of the impeller increases. This is due to the increase in the pressure driving force generated by the impeller. The impeller relative velocity has a direct impact on the gas induction rates. The submersion height of the liquid one of the most important factor which in determining the gas induction rate in a gas inducing mechanically agitated contactors. The equation which is given below for induction rate was fairly successful in predicting the gas induction rate for a variety of different operating conditions^{2,4,7}.

$$Q_1G = C_{1o} A_{1o} \sqrt{(\rho_1(L(1-\epsilon))/\rho_1G + \epsilon) C_{1p}(\theta)[2\pi RN(1-K)^2 - (2\rho_1LgS)/\rho_1G]} \quad (1)$$

From the above equation it is clear that the liquid height over the impeller and the rotational speed of the impeller has an influencing effect on the gas induction rates. The model which is given in the equation (2) indicate that the effect of submersion depth on the gas induction rate³.

$$Q_G = S \sqrt{\left[\frac{\rho_L(1-\epsilon_g)}{\rho_g} + \epsilon_g \right] [(\pi d_d NK)^2 + 2h_{f1} - 2h_g] - 2h_{f2}} \quad (2)$$

2.3 Gas holdup

The gas holdup in the gas inducing mechanically agitated contactors will increase as the submersion depth increases^{3,14}. This may be due to the increased bubble residence time in the liquid. The work is also pointing out that the size of the induced bubbles found reducing as the liquid height over the impeller reduces. The smaller bubbles always find greater residence time in liquid due to its higher density related to the larger bubbles.

2.4 Power consumption

The power consumption increases with the increase in the gas induction rate in the gassed state of the working liquid^{9,11}. Higher rotation speeds only can generate higher gas induction rates in a gas inducing mechanically agitated contactor and will result to the higher power consumption⁶.

3. Experimental Setup

The main constituent of the experimental setup was a transparent baffled tank fixed on a stand provided with a sparger at the bottom of the tank. The other major components of the setup are the hollow impeller and the hollow shaft. One end of the shaft was mounted to a bearing on the bottom of the tank and other end was connected to the coupling which extends the it to a mechanical drive served by a 2 hp 3 phase delta motor. The hollow impeller with the orifices was mounted on the shaft and the orifices were on the top of the blade surface. The schematic diagram of the impeller is given in the figure 2. A stator which is fixed at the top of the tank extending in to the working liquid. This was to restrict the flow of the induced air through the respective gas

flow meter. The induction line had been made sufficiently large in diameter to make the pressure drop due to the friction is negligible. The compressed air for the sparger was generated by a 1hp compressor and is entered through a gas flow meter and a stop cock into the sparger. The liquid level in the tank is measured from the scales which situated at half way in the circumferential distance between the baffles and are four in number. The rotational speed of the impeller was measured using a digital tachometer and the rotational speed is controlled by frequency modulation electric drive control. The power consumed by the electric motor was measured using dual watt meter method by employing digital watt meters. The power consumption for the generation of the sparged air was calculated on the basis of the volume transferred during the process. The volumetric flow rate of the induced gas and the sparged gas were measured using the air flow meters fitted in the respective lines. The schematic diagram of the experimental setup is given in the figure 2 and the specifications of the setup are available with table 1.

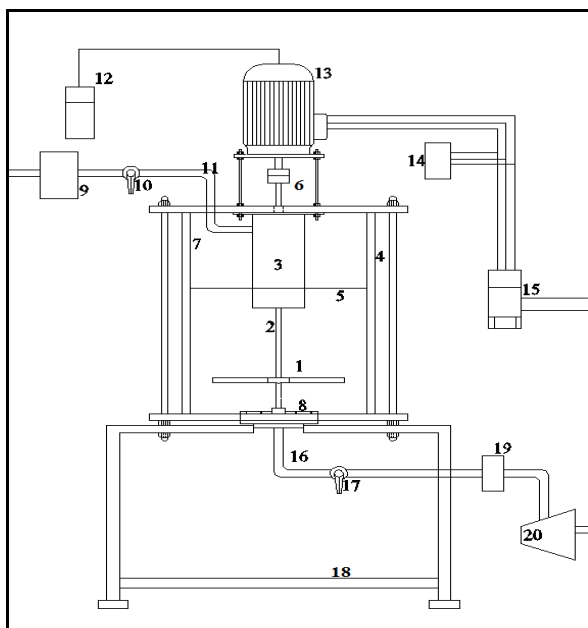
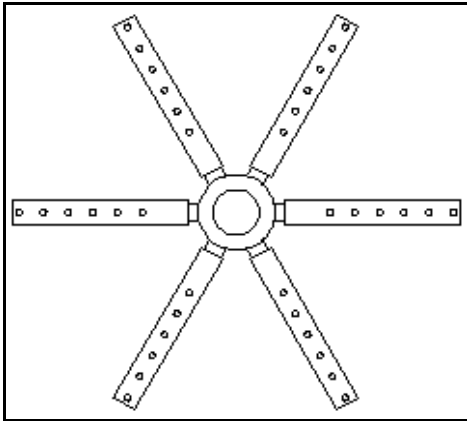


Figure 2: Experimental setup.

1. Hollow turbine impeller
2. Hollow shaft
3. Stator pipe
4. Transparent Tank
5. Liquid level
6. Drive coupling
7. Baffle
8. Air Sparger
9. Air flow meter for induced air
10. Stop cock
11. Line for air induction
12. Tachometer setup
13. Drive motor
14. Watt meter setup for power measurement
15. Frequency modulation electric drive controller
16. Line for sparging air
17. Stop cock
18. Equipment stand
19. Air flow meter and regulator for sparged air
20. Compressor

Table 1: System specification (All dimensions are in mm)

Tank and hollow shaft		Straight blade turbine type hollow impeller			
Tank diameter	450	Impeller diameter	150	Orifice diameter	2
Tank depth	570	Impeller hub internal diameter	25	Number of orifices	6
Number of baffles	4	Impeller hub external diameter	15	Inter orifice distance	8
Baffle width	40	Impeller blade height	30	Impeller blade thickness	8
External diameter of shaft	15	Number of blades	6	Blade channel diameter	4
Internal diameter of shaft	8	Effective blade length	60	Total number of orifices	42
Air sparger					
Diameter	150	Orifice diameter	2	Type	Fixed
Number of orifices	42	Orifice polar array	6x7	Location in the tank	Bottom

**Figure 3: Top view of the hollow turbine impeller**

4. Experimentation

In the experimentation, the system had been studied in two different ways to make the comparison of the power consumption. The former when the system was in the induction mode and the latter was in the sparging mode. In order to make the system in the induction mode the stop cock in the sparging line had been shut and the same in the induction line kept open. As the impeller started to rotate the gas started to enter into the liquid through orifice. The flow rate of the induced gas was measured by the gas flow meter in the induction line. The height of the diphasic fluid after the induction and the initial height of the liquid could be measured from the scales fixed on the tank. These heights could be converted in to the fractional gas holdup using the following equation.

$$\varepsilon = \frac{h_2 - h_1}{h_1} \quad (3)$$

The power consumption for the process was calculated from the watt meters and the rotation speed of the shaft is measured was measured from the digital tachometer. During the entire experimentation water had been used as the working fluid and the bottom clearance of the impeller was maintained as 50mm. The submersion depths are varied from 150mm to 300mm at an increment of 50mm. The gas holdup, the power consumption and the induced gas flow were measured for all the four submersion depths.

In order to make the setup to run in the sparging mode the stop cock in the sparging line was kept open and the same in the induction line was kept closed. The closing of the induction line stop cock prevented the induction of the air in to the liquid. The gas sparging rate was set equal to the gas induction rate at corresponding rotational speed. All other conditions in the system has been kept same as of the induction experiment made for a particular submersion depth including the rotation of the impeller. The required

parameters were measured for the four different submersion depths. The power consumption for the sparging mode will be different with the induction mode. In the sparging mode the power consumption will be the sum of the power consumption of the motor for the rotation of the impeller and the power consumed for the generation of the compressed air for the sparging.

5. Results and discussion

5.1. Effect of rotational speed on the rate of gas induction

The rpm of the impeller has a direct relation with the gas induction rate in an inducing mechanically agitated contactor. It has been observed throughout the experimentation that an increased gas induction rate only can be accomplished with an increased rotational speed of the impeller. This due to the increased pressure reduction in the liquid by creating higher impeller slip factor with respect to the increment in the rotational speed. It has been observed that the rate of gas induction was increased as the rotational speed increased for various impeller immersion depths. The figure 4 indicates the relation between the induction rate and the rotational speed.

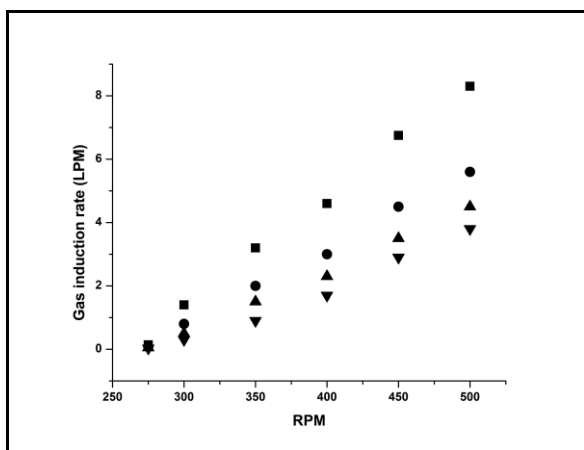


Figure 4- Effect rotational speed on gas induction rate for different impeller immersion depths of (■)20cm, (●)25cm, (▲) 30cm and (▼)35cm

The power consumption for higher induction rates are high because the higher rotational speeds require higher power. The figure 5 indicates the relation of the gas induction rates with the power consumption.

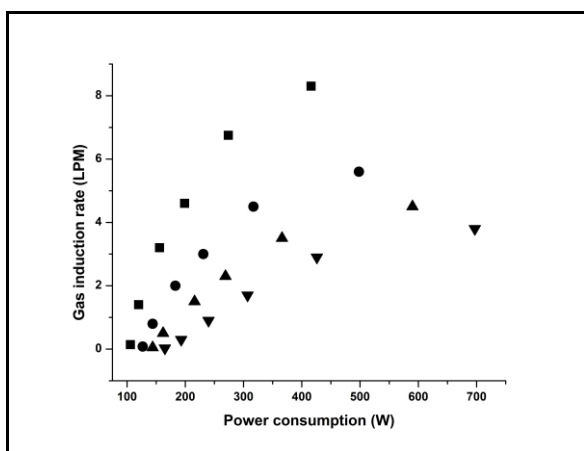


Figure 5- Relation of gas induction rate and power consumption at impeller immersion depths of (■)20cm, (●)25cm, (▲) 30cm and (▼)35cm

5.2. Effect of submersion depth on the rate of gas induction

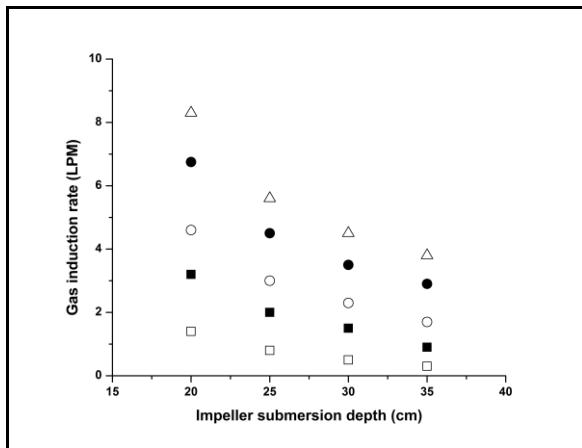


Figure 6 - Relation of gas induction rate with impeller submersion depths at (□)300 rpm, (■)350 rpm, (○)400 rpm, (●)450 rpm, (▼)500 rpm

The submersion depth is the most important non geometrical criteria which determine the gas induction rates. In the experimentation it has been observed the gas induction rate has been decreases with the increase in the immersion depths. As the impeller submersion depth increases the static pressure offered by liquid present in the tank increases. So the pressure has to be overcome by the impeller rotation increases so the gas induction rate decreases. The power consumption for the same rate of gas induction also increases for the higher submersion depths. The figure 6 indicates the relation of gas induction rate with impeller submersion depths at various rotational speeds.

5.3. Effect of submersion depth on the gas holdup

In the experimentation the submersion depth increased the gas holdup also increased. This may be due to two reasons. The first one is the increased submersion depth would be resulting in the increased liquid depths. So at the increased liquid depths the retention time of the bubbles would have been increased in the gassed state of the working liquid. A higher bubble retention time could have brought a higher gas holdup. The second reason is that at higher submersion depths the same induced gas flow rates could be achieved by comparatively higher rotational speeds of the impeller. The higher rotation of the impeller would provide increases bubble breakage and better dispersion of the induced gas bubbles. The better dispersion and the smaller bubble size can increase the retention time of the gas bubbles and thus the gas holdup in the gassed state. The figure 7 indicates the relation between the has holdup and the submersion depth.

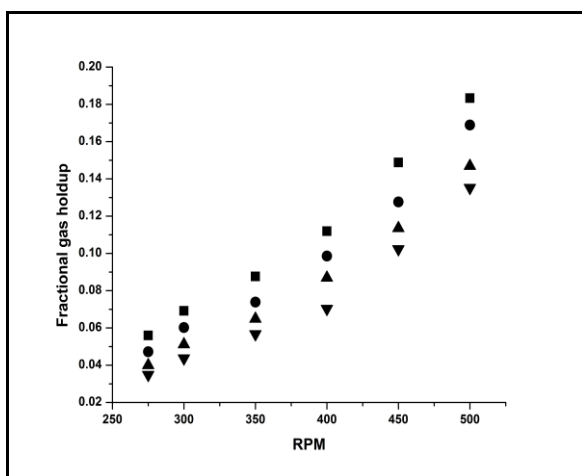


Figure 7 - Relation between the gas holdup and rotational speed at various submersion depths of (■)20cm, (●)25cm, (▼)30cm, (▲)35cm

5.4. Comparison of the power consumption

It has been observed in the experimentation that the power consumption by the induced process was lower than a sparged process. This was due to extra power consumed by the air compressor for generating the compressed air for sparging. The induction process did not have an air compressor in the external loop so the power consumption by the induction process was less compared to the sparging process at different process conditions. The figure 7 relates the fractional gas holdup with the power consumption which justifies the above aspect.

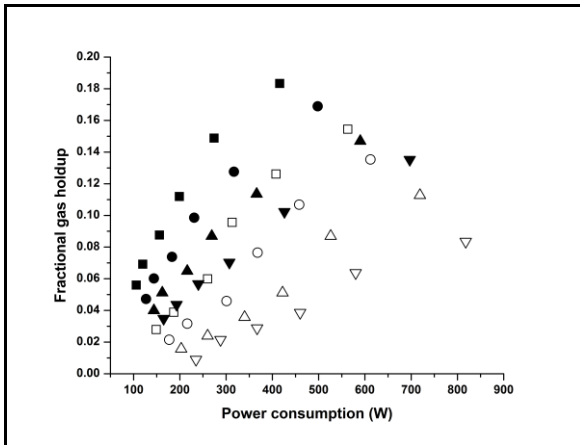


Figure 7 - Relation between fractional gas holdup and power consumption at various immersion depths of 20cm (□)sparging and(■)induction, 25cm (○)sparging and (●)induction, 30cm (△) sparging and (▲)induction, and 35cm (▽)sparging and (▼)induction.

5.5. Comparison of gas holdup of induced process to the sparged process

In the experimentation the induced process always achieved a higher gas holdup as compared to the sparged process. This due to smaller size of the bubbles formed during the induction process as compared to the size of the bubbles formed by sparging. The size of the induced bubbles was less compared to the bubbles produced in the sparged process and the size reduction of the induced bubbles to a higher extend had also been observed as compared to the sparged bubbles. In the figure 8 and 9 indicates the relation of fractional gas holdup with the gas flow rate and the rotational speeds. This depicts the improved performance of the gas inducing mechanically agitated contactor in comparison with the gas sparging mechanically agitated contactors.

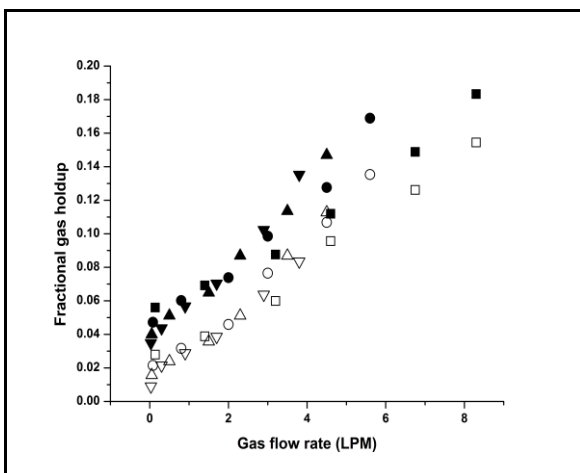


Figure 8 - Relation between fractional gas holdup with gas flow rate at various immersion depths of 20cm (□)sparging and(■)induction, 25cm (○)sparging and (●)induction, 30cm (△)sparging and (▲)induction and 35cm (▽)sparging and (▼)induction.

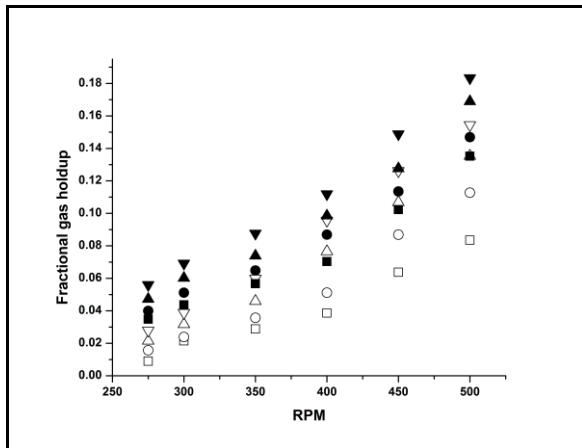


Figure 9 - Relation between fractional gas holdup with rotational speed at various immersion depths of 20cm (□)sparging and(■)induction, 25cm (○)sparging and (●)induction, 30cm (△)sparging and (▲)induction, 35cm (▽)sparging and (▼)induction.

6. Conclusion

In the induction process if GIMAC, the gas flow rate is having a direct relation with the rotational speed of the impeller. The impeller speed increased the induced gas flow rate increased. The impeller submersion depth is also holding highly influencing effect on the gas induction rate and the fractional gas holdup. The higher submersion depth will result in the lower gas induction rates and higher gassed state gas holdup. The higher rate of gas flow also can bring a higher gassed state gas holdup. The comparison of the GIMAC with the gas sparging type revealed that the former is having better performance edge over the latter in terms of power consumption and gassed state gas holdup.

Nomenclature

- A_o = Area of the orifice, m^2
 C_d = Orifice drag coefficient. Dimensionless
 C_o = Impeller orifice discharge coefficient
 $C_p(\theta)$ = Pressure loss coefficient or pressure coefficient
 g = Acceleration due to gravity, m/s^2
 H = Total liquid height, m
 h_{f1} = Energy loss in the turbulent field, J/kg
 h_{f2} = Energy loss during the gas flow, J/kg
 h_1 = Initial liquid height read from the scale
 h_2 = Liquid height in the gassed state from the scale
 K = Slip factor between impeller and the fluid or speed loss coefficient
 N = Impeller rotational speed, rps
 N_{CG} = Onset gas induction speed, rps.
 P_o = Head space pressure, N/m^2
 $P[\theta]$ = Pressure at any angular location at the impeller blade, N/m^2 .
 Q_G = Gas induction rate m^3/s
 S = Submersion depth of the impeller orifice in the liquid, m
 ϵ = Fractional gas hold up in the working medium
 ϵ_g = Fractional gas holdup
 θ = Attacking angle of the impeller blade.
 ρ_L = Density of the liquid, kg/m^3

References

1. Ashwin W. Patwardhan and Jyeshtharaj B. Joshi., Design of Gas-Inducing Reactors, Industrial Engineering and Chemistry Research Journal,1999, 38, 49-80.
2. Evans.G.M, Rielly.C. D, Davidson, J. F, Carpenter. K. J., Hydrodynamic Characteristics of a Gas-Inducing Impeller, Proceedings of the 7th European Conference on Mixing, Kiav, Brugge, 1991,18-20, 515-523.
3. Fan Ju, Zhen-Min Cheng, Jian-Hua Chen, Xiao-He Chu, Zhi-Ming Zhou and Pei-Qing Yuan, A novel design for a gas-inducing impeller at the lowest critical speed, Chemical Engineering Research and Design Journal, 2009, 87,1069-1074.
4. Joshi, J. B., Modifications in the Design of Gas Inducing Impellers, Chemical Engineering Communication Journal, 1980, 5 (1-4), 109-114.
5. Joshi, J. B and Sharma, M. M., Mass Transfer and Hydrodynamic Characteristics of Gas Inducing Type of Agitated Contactors, Canadian Journal of Chemical Engineering and Technology, 1977, 65, 683-95.
6. Kaliannagounder Saravanan, Vishwas D. Mundale, Ashwin W. Patwardhan, and Jyeshtharaj .B. Joshi, Power Consumption in Gas-Inducing-Type Mechanically Agitated Contactors, Industrial and Engineering Chemistry Research Journal, 1996, 35,1583-1602
7. Martin, G. Q, Gas-Inducing Agitator, Industrial and Engineering Chemistry Process Design and Development Journal. 1972, 11, 397-404.
8. Raidoo, A. D, Raghav Rao, K. S. M. S, Sawant.S. B and Joshi. J. B., Improvements in a Gas Inducing Impeller Design, Chemical Engineering Communication Journal, 1987, 54, 241-64.
9. N. A. Deshmukh, S. S. Patil and J. B. Joshi, Gas induction characteristics of hollow self-inducing impeller, Chemical Engineering Research and Design Journal, 2006, 84(A2), 124–132.
10. Rielly, C. D, Evans.G.M, Davidson.J. F and Carpenter. K. J, Effect of Vessel Scale-up on the Hydrodynamics of a Self-Aerating Concave Blade Impeller, Chemical Engineering Science Journal, 1992, 47, 3395 3402.
11. Saravanan. K, Mundale. V. D, and Joshi. J. B, Gas Inducing Type Mechanically Agitated Contactors, Industrial Engineering and Chemistry Research Journal, 1994, 33, 2226-2241.
12. S.E. Forrester and C.D. Rielly, Modeling of increased gas capacity of self inducing impellers, Chemical engineering science Journal, 1994, 49, 5709-5718.
13. S.E Forrester, CD Rielly and KJ Carpenter, Gas inducing impeller design and performance characteristics, Chemical engineering science Journal, 1998, 56, 603-615.
14. C. Gomadurai, K. Saravanan, Eldho Abraham and N. Deepa, Hydrodynamic Studies on Air Inducing Impeller Systems, International Journal of Chem Tech Research, 2014, 6, 4471-4474.



www.technochemsai.com